



## A highly efficient InGaP thin film solar cell structure, optimization and characteristics

Fatiha Djaafar<sup>1,2✉</sup>, Baghdad Hadri<sup>2</sup>

<sup>1</sup>Laboratoire de Développement Durable de l'Energie Electrique (LDDEE), Electrotechnical Department, University of Sciences and Technology of Mohamed Boudiaf (USTOMB), Oran, Algeria

<sup>2</sup>Electromagnetism and Guided Optic Laboratory, Department of Electrical Engineering, University of Abdelhamid Ibn Badis, 27000 Mostaganem, Algeria

Received August 15, 2021

Revised May 9, 2022

Accepted September 5, 2022

Published online: January 31, 2024

### Keywords

InGaP Solar cell

Window

Efficiency

Open circuit voltage

Optimization

Simulation

**Abstract:** Inorganic solar cells based on III-V semiconductor materials are widely used owing to their high efficiencies. In this work, we aim to improve the performance of the single heterojunction solar cell InGaP. The InGaP cell is constituted of a back surface field (BSF), a base, an emitter and a window layer with InAlAsP material. The simulation is done after optimization, modeling, and choice of the used materials and the thickness of different layers constituting the solar cell. The choice of materials whose gap energy is decreasing allows the absorption of the solar spectrum in its almost totality. Then, we varied the temperature to know its effects on the gap energy and the efficiency of the InGaP cell. The InGaP and solar cell with optimal parameters are illuminated by an AM1.5 solar spectrum through InAlAsP window layer. The simulation and optimization at 300K of short circuit current parameters ( $J_{sc}$ ), open circuit voltage ( $V_{oc}$ ), fill factor (FF) and efficiency ( $\eta$ ) are done using Tcad Silvaco software. The characteristics obtained are: the minimized thickness of 665 nm, electrical efficiency is about  $\eta = 21.87\%$  for InGaP cell,  $J_{sc} = 14.43 \text{ mA/cm}^2$ ,  $V_{oc} = 1.63 \text{ V}$ , and  $FF = 91.21\%$ .

© 2023 The authors. Published by Alwaha Scientific Publishing Services, ASPS. This is an open access article under the CC BY license.

## 1. Introduction

Photovoltaic solar energy is in development and the research is very active in the domain during these last years because it provides the following advantages: the abundance in nature and non-pollution. The production of electrical energy is the direct transformation of solar energy (illuminated rays) into electrical energy. The principal base of this transformation is the solar cell or precisely the semi-conductors which constitute this cell.

The amelioration of solar cell efficiency requires the amelioration of the procedures (mechanisms) of the production of solar cells and in particular the suitable choice of materials. The choice is based on alloying

semiconductors whose lattice constant is equal. An essential response to decrease the losses and ameliorate the efficiency of photovoltaic cells is known from a technological view is stacking materials possessing decreasing gap energy (heterojunctions) to obtain a structure with optimal characteristics.

The indium gallium phosphide (InGaP) is one of the primordial materials in thin film technology production. In this context, we aim to simulate an InGaP heterojunction cell to achieve maximum efficiency.

The optimization of an InGaP solar cell and its performance has been widely investigated by many authors. In recent studies, Benlekhdem et al. (2018) gave

\* Corresponding author. E-mail address: [fatiha.djaafar@univ-usto.dz](mailto:fatiha.djaafar@univ-usto.dz)

the structural parameters and modeling of InGaP solar cells with an efficiency of 18.55% at AM1.5 sun. The proposed structure possessed a thickness of 850nm.

This work consists of introducing several parameters characterizing the multi-layer cell, in particular, the thickness (thin film technology); the type of materials used which gives a high efficiency as well as the thickness of the Back Surface Field (BSF) layer.

Generally, inorganic cells are used in space applications. These materials are costly. So, they must be thin and performant at the same time. The internal characteristics of the used materials, concentration and thickness, and the external parameters such as temperature affect negatively the InGaP electrical characteristics and decrease their efficiency as mentioned by Mekemeche (2017). The aim to decrease the thickness of the InGaP single cell and increase its performance gives major importance to this study.

In this paper, we modeled and optimized the InGaP solar cell based on III-V inorganic materials. We have extracted the characteristics of merit: short circuit current parameters ( $J_{sc}$ ), open circuit voltage ( $V_{oc}$ ), fill factor (FF), and efficiency ( $\eta$ ). This work aims also to optimize the properties of InGaP cell structure and to simulate this optimized design. This paper includes also optimization of the effect of certain layers as substrate, window layer, and BSF on InGaP cell performance.

## 2. Physical models

The models used in the simulation of proposed structures are: The recombination model in volume is: radiative, Auger, Shockley Read Hall (SRH), and recombination in surface, arsenic diffusion was included to act as a back surface field (BSF), reducing recombination at the back surface.

### 2.1. Trap-assisted recombination

Radiative and non-radiative recombinations depend on doping, whereas SRH recombination depends on defects located on deep trapping levels.

### 2.2. Recombination SRH (Shockley-Read-Hall)

The Shockley-Read-Hall recombination process will take place within near-mid-gap energy level (traps) as shown in Fig. 1. It is due to the presence of impurities or defects in the crystal lattice. The electron jumps from the conduction band to an intermediate energy level, then jumps a second

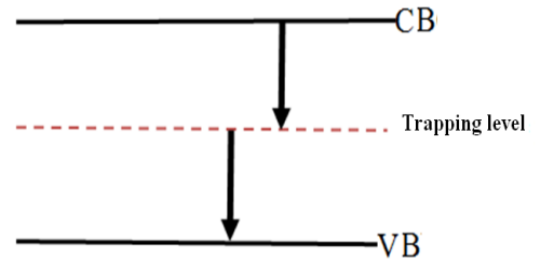


**Fig. 1:** Descriptive diagram of the recombination by trap process.

time to the valence band which recombines with a hole. The process of SRH depends mainly on the density of deep levels and therefore the quality of the material. Shockley-Read-Hall recombination is given by the following equation cited in Manual (2012) and Zeghbrouck (2007).

$$R_{SRH} = \frac{pn - n_{ie}^2}{\tau_{p0} \left[ n + n_{ie} \exp\left(\frac{E_t - E_i}{KT_L}\right) \right] + \tau_{n0} \left[ p + n_{ie} \exp\left(\frac{-(E_t - E_i)}{KT_L}\right) \right]} \quad (1)$$

Where:

$E_t$ : energy position of trap states.

$E_i$ : fermi level in the intrinsic semiconductor

$\tau_{n0}$ : lifetime of the electrons

$\tau_{p0}$ : lifetime of the holes.

$n_{ie}$ : intrinsic concentration

$K$ : Boltzmann constant.

$T_L$ : temperature in Kelvin.

$$\tau_n = \frac{\tau_{n0}}{1 + N/N_{SRHN}} \quad (2)$$

$$\tau_p = \frac{\tau_{p0}}{1 + N/N_{SRHP}} \quad (3)$$

$N_{SRHN}$  and  $N_{SRHP}$  are parameters specifying the SRH concentration for electrons and holes.

$N$ : local (total) concentration of impurity,

### 2.3. Surface recombination

The recombination process SRH is generally expressed in terms of recombination per unit area and not per unit volume according to the following relationship given in Manual (2012) and Marouf (2013):

$$R_{surf} = \frac{pn - n_{ie}^2}{\tau_p^{eff} \left[ n + n_{ie} \exp\left(\frac{E_t - E_i}{KT_L}\right) \right] + \tau_n^{eff} \left[ p + n_{ie} \exp\left(\frac{-(E_t - E_i)}{KT_L}\right) \right]} \quad (4)$$

$$\frac{1}{\tau_p^{eff}} = \frac{1}{\tau_p} + \frac{d_i}{A_i} S_n \quad (5)$$

Where:

$\tau_n^{\text{eff}}$ : Effective lifetime.

$d_i$ : Interface length.

$A_i$ : Thickness of the interface.

$S_n$ : Recombination rate for electrons.

$S_p$ : Recombination rate for holes.

$S_n = S_p = 0$  cm/s.

$\tau_n^i$  and  $\tau_p^i$ : the lifetime of electrons and holes calculated at a node  $i$  through an interface.

## 2.4. Volume recombination of Auger type

Auger recombination consists of a transfer of electron energy from the valence band as kinetic energy to another free electron. This energy is released in form of phonons. This process will take place in heavily doped regions and requires at least one electron and one hole as mentioned by Zeghbrouck (2007) and Bali (2013) and shown in Fig. 2:

Auger recombination is modeled in Manual (2012) according to the following expression

$$R_{\text{Auger}} = \text{Aug}_n(pn^2 - nn_{ie}^2) + \text{Aug}_p(np^2 - pn_{ie}^2) \quad (6)$$

Where  $\text{Aug}_n$  and  $\text{Aug}_p$ : Auger coefficients for electrons and holes and specifically for each material.

## 2.5. Radiative recombination

Radiative recombination is defined as the recombination of an electron from the conduction band with a hole in the valence band as shown in Fig. 3. According to Mallem (2014), it appears in direct gap materials like GaAs and is less used by indirect gap materials such as Si.

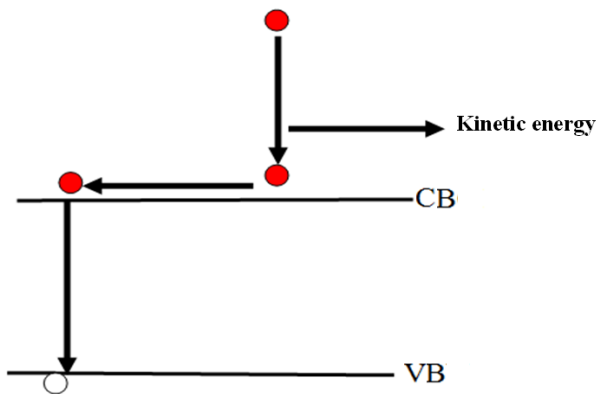


Fig. 2: Auger recombination mechanism.

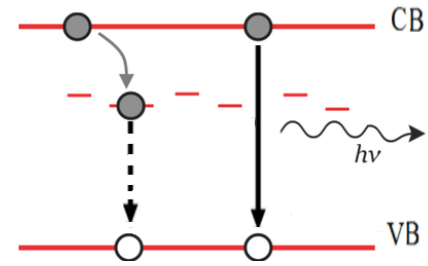


Fig. 3: The radiative recombination process.

## 3. The choice of InGaP cell structure

### 3.1. Choice criteria

The alloying of semiconductor materials such as InGaP depends on the physical and electronic properties of each semiconductor. The semiconductor alloy is the main step to simulate and realize a single junction solar cell. In our case, we took into account the properties of the semiconductor: InGaP.

In this work, we have used alloys of III-V semiconductors as the  $\text{In}_{(1-x)}\text{Ga}_{(x)}\text{P}$  because they ensure high efficiency. The calculation of some parameters in a ternary alloy  $\text{A}_{(x)}\text{B}_{(1-x)}\text{C}$  is given by the linear equation (called the Vegard law) taken from Manual (2012).

Gap energy: the value of the gap energy that allows the absorption of the AM1.5 spectrum varies from 1.75 to 1.8 eV for InGaP cell. Mahfoud (2015) has calculated the gap energy of InGaP cell is 1.90eV

The lattice constant: the epitaxy (heterojunction) of the two different semiconductors can only be done if the semiconductors have very close lattice constants to avoid the mismatch between the substrate and the semiconductor material.

The lattice constant of  $\text{In}_{(1-x)}\text{Ga}_{(x)}\text{P}$  (a ternary alloy) is calculated according to Vegard's law as follows:

The lattice constant of  $\text{In}_{(1-x)}\text{Ga}_{(x)}\text{P}$  (a ternary alloy) is calculated according to Vegard's law as follows

$$[10]: \alpha_{\text{In}_{(1-x)}\text{Ga}_{(x)}\text{P}} = x\alpha_{\text{GaP}} \quad (7)$$

Where  $\alpha$  is the lattice constant and  $x$  is the molar fraction. Table 1 summarizes the network constants of the material used.

Table 1. Materials Lattice constant

Materials	InGaP	GaAs	InAlAsP	AlGaAs
Lattice constant (Å)	5.65	5.65	5.65	5.65

**Table 2.** Material properties  $\text{Ga}_x\text{In}_{1-x}\text{P}$  at 300 K.

Parameter	$\text{Ga}_x\text{In}_{1-x}\text{P}$	$\text{Ga}_{0.5}\text{In}_{0.5}\text{P}$
Gap energy (eV)	$E_g(x)=1.35+0.73x+0.7x^2$	1.89
Dielectric permittivity $\epsilon$	$12.5-1.4x$	11.8
Electronic affinity	$\chi(x)=4.38-0.58x$	4.09
$\kappa$ (eV) Auger coefficient	$A(x)=-8.2 \times 10^{-30}x^2 + 8.3 \times 10^{-30}x + 9 \times 10^{-31}$	$8.3 \times 10^{-30} \text{ (cm}^6/\text{s)}$
Radiative recombination	$A_0(E_g) = (1 \pm 0.3) \times 10^{-10}$	$A_0 \text{ (cm}^3/\text{s)}$
Effective mass of electrons and holes	$\frac{m_e^*(x)}{m_0} = 0.0254x^2 - 0.114x + 0.08$	$\frac{m_e^*(x)}{m_0} = 0.029$
$m_e^*(x)$ and $m_h^*(x)$	$\frac{m_h^*(x)}{m_0} = 0.19x + 0.6$	$\frac{m_h^*(x)}{m_0} = 0.695$

### 3.2. Properties of InGaP

All The  $\text{Ga}_x\text{In}_{1-x}\text{P}$  is a ternary compound. It has a direct gap for a molar fraction less than 0.74 and an indirect gap for a molar fraction greater than 0.74. It is characterized by a low rate of recombination on the surface. Djaafar (2018) has shown the material properties of  $\text{Ga}_x\text{In}_{1-x}\text{P}$  at 300k in Table 2.

### 4. Simulation results

We interpreted the simulation results obtained as short-circuit current ( $J_{sc}$ ), open-circuit voltage ( $V_{oc}$ ), fill factor (FF), and efficiency ( $\eta$ ) as the effects of different geometric and electrical parameters on the performance of the optimized cells such as thickness, window layer, BSF and temperature on the solar cell output.

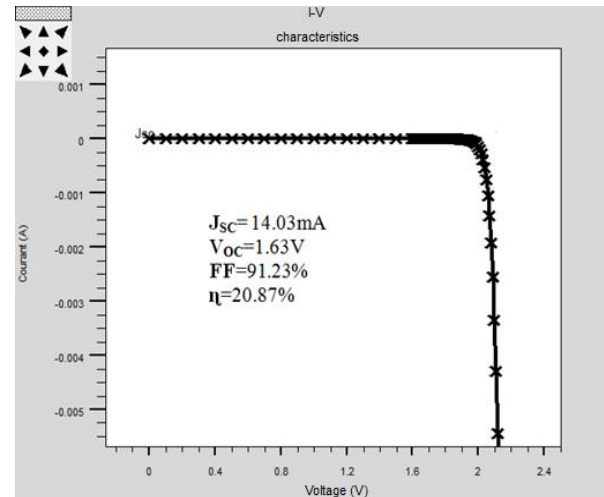
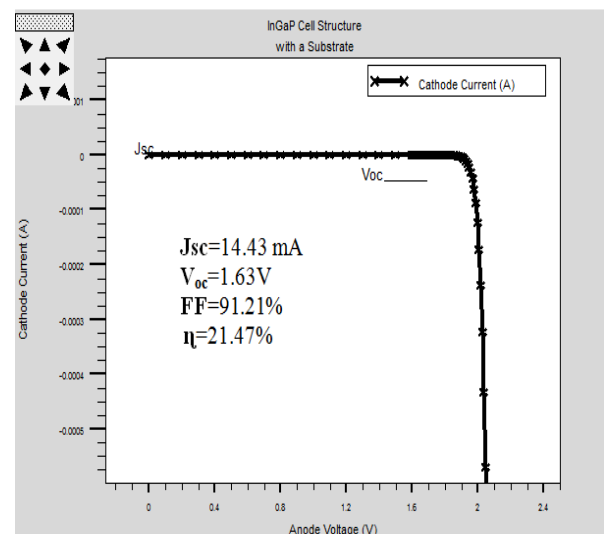
#### 4.1. Cells structure

The InGaP mono junction solar cell consists of four layers: a window, emitter, base, and a BSF. The parameters of the optimized cell are shown in Fig. 4.

#### 4.2. Device Modeling

The optimized InGaP cell structure was simulated using Silvaco-Atlas. We have first optimized the parameters of the proposed structure such as the materials, the thickness, and doping concentration. Then, we have, simulated this configuration to extract the characteristics of merit such as open circuit voltage ( $V_{oc}$ ), short circuit current ( $J_{sc}$ ), fill factor, and efficiency.

anode contact			
30nm	Window	n+InAlAsP	accept=1e19cm-3
55nm	Emitter	n+InGaP	accept=15e18cm-3
550nm	Base	P+ InGaP	donors=11e18cm-3
30nm	BSF	p+ InAlAsP	donors=10e19cm-3
30nm	Substrate	p+InAlGaP	donors=2e18cm-3
cathode contact			

**Fig. 4:** Optimized InGaP cell design.**Fig. 5:** InGaP cell I-V characteristics without a substrate.**Fig. 6:** InGaP cell I-V characteristics with a substrate.

The InGaP solar cell is simulated with the characteristics mentioned in Table 2 and the thickness proposed in the structure. In the first stage, we simulated the structure without a substrate, and then with it. The simulation results obtained are shown in Figs. 5 and 6, respectively.

We notice that the substrate is a passive component but it may have an important role in improving the efficiency of the cell. According to Terghini (2020), for a thin-film solar cell that requires high-temperature processing of thin films, a suitable glass or ceramic substrate is used.

#### 4.3. The effect of a window layer on the efficiency of the cell

The choice of the thin and highly doped ( $10^{19} \text{ cm}^{-3}$ ) "InAlAsP" window layer is chosen taking into consideration certain criteria such as the gap energy ( $E_g$ ) which must be greater than that of the InGaP emitter and it must produce a speed of weak surface recombination.

The InGaP solar cell is simulated without the window layer, and the I-V characteristic is illustrated in Fig. 7. The values of the short-circuit current ( $J_{SC}$ ), open circuit voltage ( $V_{OC}$ ), the form factor (FF) and the efficiency ( $\eta$ ) are respectively:  $J_{SC} = 12.61\text{mA}$ ,  $V_{OC} = 1.40\text{ V}$ ,  $FF = 90.40\%$ , and  $\eta = 15.98\%$ .

Thus, the window layer allows the electrons to flow to the electrical contacts without increasing the resistance of the cells in series and increases the efficiency of the cell. The window layer avoids surface recombination and solves the problem of mesh mismatch [15].

#### 4.4. Effect of temperature on the efficiency

With an increasing operating temperature of the solar cell, we noticed an increase in  $J_{SC}$ , a decrease  $V_{OC}$ , and hence a decrease in efficiency. The table.3 summarizes the different variations of  $J_{SC}$ ,  $V_{OC}$ ,  $P_{Max}$ ,  $\eta$ , and FF with the variation of the temperature.

We have simulated the single solar cell InGaP at 300, 325, 350, and 375 °K. The results of Table 3 show that the efficiency decreases by 2% for each 25 °K increase in temperature. The curves of variation of characteristics of merit ( $P_{Max}$ ,  $J_{SC}$ , FF, and  $V_{OC}$  &  $\eta$ ) as a function of temperature are shown in Figs 8, 9, 10, and 11, respectively.

**Table. 3.** Variation in characteristics of merit as a function of temperature.

	$J_{SC}(\text{mA})$	$V_{OC}(\text{V})$	$P_{max}(\text{w})$	$\eta(\%)$	FF (%)
Temperature (K)	InGaP	InGaP	InGaP	InGaP	InGaP
300	14.34	1.63	2.21	21.47	91.24
325	14.3422	1.59	2.09	20.90	91.10
350	14.3478	1.53	1.98	19.75	89.78
375	15.55	1.39	1.95	19.48	90

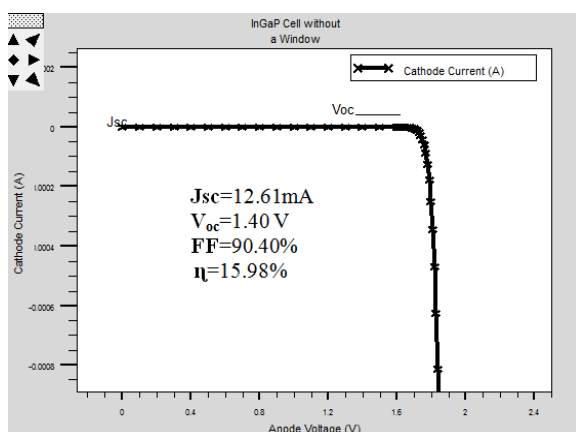


**Fig. 7:** InGaP solar cell simulation without the window layer.

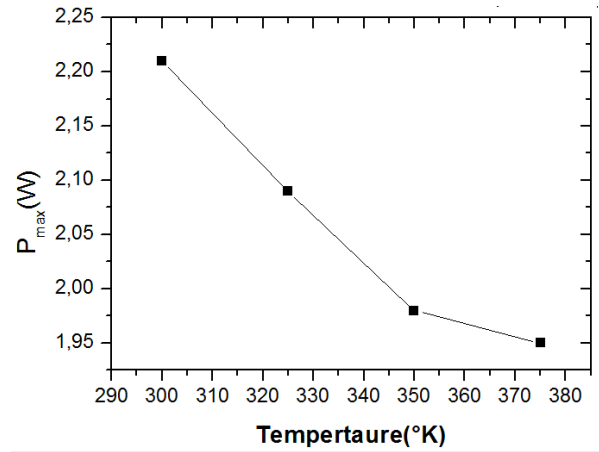


**Fig. 8:** Variation of  $P_{max}$  as a function of temperature.

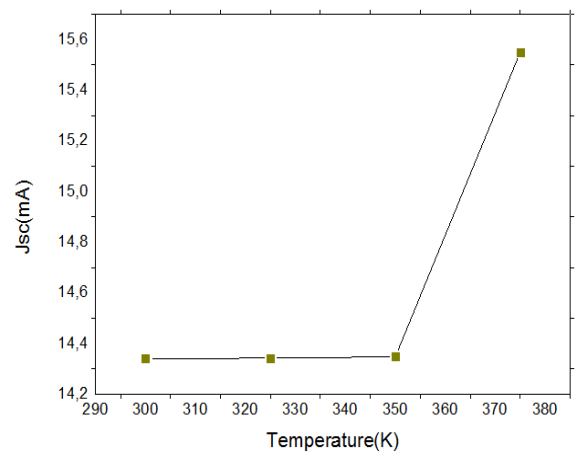


**Fig. 9:** Variation of  $J_{SC}$  as a function of temperature.

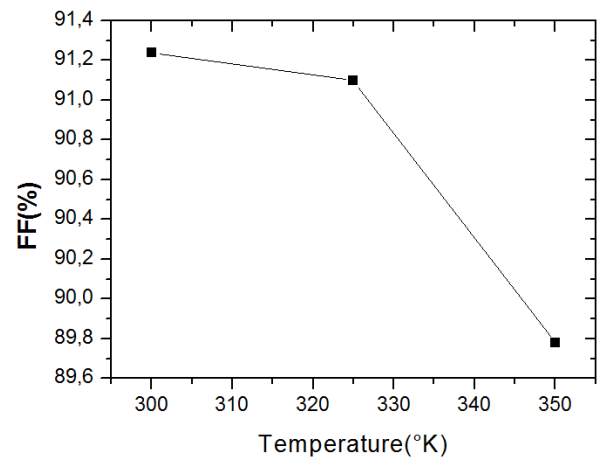


**Fig. 10:** Variation of FF as a function of temperature.

The solar cell performance was negatively affected by increasing temperature. This is done due to the increase of the resistivity with the temperature. Higher operating temperatures cause a decrease in  $V_{OC}$  at a significant rate.

For most materials, the band gap decreases with increasing temperature.

The variation of the temperature affects the band gap of the semiconductor and creates a slight increase in  $J_{sc}$  and a decrease in  $V_{oc}$  and hence a reduction in the efficiency.

According to Mahfoud (2015) and Green (1982), the following equation illustrates the semiconductor's band gap energy as a function of temperature

$$E_g(T) = E_g(0) - \frac{\alpha T^2}{T + \beta} \quad (8)$$

Where  $E_g(0)$  is the band gap energy at zero temperature,  $T$  is the temperature, and  $\alpha$  and  $\beta$  are the coefficients empirically determined for each semiconductor

Hence, the decrease of  $V_{oc}$  affects the InGaP solar cell efficiency according to the following equation

$$\eta = \frac{FF \times J_{sc} \times V_{oc}}{P_{in}} \quad (9)$$

Where  $J_0$  is the saturation current density,  $\eta$  is the efficiency,  $FF$  is the ideality factor, and  $k$  is the Boltzmann constant.

The decrease in efficiency and the maximum power of the solar cell is mainly due to the decrease in the open circuit voltage. Quoizola (2007) has calculated the variation of the maximum power as a function of the temperature in accordance with the following expression.

$$\frac{dP_{mp}}{dT} = V_{mp} \cdot \frac{dI_{mp}}{dT} + I_{mp} \cdot \frac{dV_{mp}}{dT} \quad (10)$$

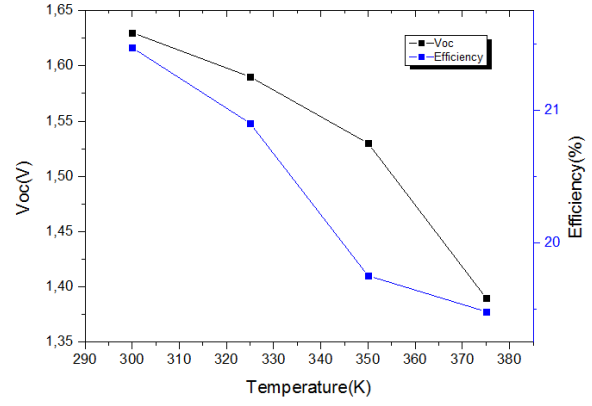
Where,  $P_{mp}$ : Maximum power;  $I_{mp}$ : Maximum current; and  $V_{mp}$ : Maximum voltage.

Figure 11 illustrates the decrease of  $V_{oc}$  of the InGaP solar cell with the increase in temperature. It achieves a minimum value of 1.39 V at 375K. Indeed, the following equation shows the variation of  $V_{oc}$  according to the temperature as expressed by Terghini (2020) and Chee & Hu (2018):

$$V_{oc} = \frac{KT}{q} \ln\left(\frac{J_{sc}}{J_0} + 1\right) \quad (11)$$

As the temperature increases, the  $FF$  decreases because of the significant decrease in voltage. We noticed a decrease of  $FF$  of 1% for each increase in the temperature of 25 ° K.

We notice a decrease in the efficiency with the decrease of  $V_{oc}$  due to the increase in temperature. It has been also proved by Mahfoud et al. (2015). High temperature narrows the band gap of the materials and then the  $V_{oc}$  above 300 K according to the Varshni equation confirmed by Manual (2012).



**Fig. 11:** Variation of efficiency as a function of temperature.

$$E_g(0) = E_{g0} - \frac{\alpha T^2}{T + \beta^2} \quad (12)$$

Where  $T$  is the temperature in Kelvin,  $\alpha$  and  $\beta$  are the coefficients of band gap temperature. They are specific for each material.

The decrease in voltage and the increase of short current density affect the short current circuit and the efficiency of InGaP solar cells according to the following equations mentioned by authors Sullivan (2010), Khan et al. (2016), and Chee & Hu (2018):

$$J_{sc} = \{I_0 [\exp\frac{qV}{KT} - 1] - I_L\} \quad (13)$$

$$\eta = \frac{FF \times J_{sc} \times V_{oc}}{P_{in}} \quad (14)$$

Where  $I_L$  is the photo-generated current and  $V$  is the photovoltage.

## 5. Conclusion

In this work, we have optimized the optimal parameters to simulate an InGaP solar cell based on inorganic materials. We have achieved an optimal structure with a thickness of 665 nm. This structure provides an efficiency of 21.87% at 300K. We have extracted the electro-optical parameters, the I-V characteristics, and the spectral response.

In this work, we were able to extract the internal and external parameters that affect the performance of the InGaP single junction solar cell such as the thickness of layers. Finally, we extracted the effect of external parameters such as temperature on the efficiency of the InGaP cell. We have illustrated that: the increase in temperature decreases the open circuit voltage, the fill factor, and the conversion efficiency of the cell.

The results obtained in this paper explain the effect of different parameters and temperatures in varying

efficiency. This study contributes to a new proposed structure with less thickness, higher efficiency, and different materials for layers.

### Nomenclature

$J_{sc}$	short-circuit current, mA
$V_{oc}$	open-circuit voltage, V
FF	fill factor, %
$\eta$	efficiency, %
$J_0$	the reverse saturation current density

### Greek symbols

$\epsilon$	Dielectric permittivity
$\chi$	Electronic affinity, eV

### Disclosures

Free Access to this article is sponsored by SARL ALPHA CRISTO INDUSTRIAL.

### References

- Bali, A. (2013). Etude Comparative entre les Cellules Solaires de Type P+-AlGaAs/ P-GaAs/N-GaAs Et Une Autre De Type N+-AlGaAs/N-GaAs/P-GaAs. Master thesis. University of Mohamed Khider – Biskra Algeria.
- Benlekhdim, A., Cheknane, A., Sfaxi, L., Hilal, H. S. (2018). Efficiency improvement of single-junction InGaP solar cells by advanced photovoltaic device modeling. *Optik*, 163, 8-15.
- Chee, K.W.A., Hu, Y. (2018). Design and optimisation of ARC less InGaP/GaAs single/multi-junction solar cells with tunnel junction and back surface field layers. *Superlattices and microstructures*. 119, 25-39.
- Djaafar, F. (2018). Etude et Modélisation des Performances des Cellules Photovoltaïques à Multi Couches à Base des Semi-conducteurs. PhD Thesis. University of USTOMB of Oran, Algeria.
- Green, M.A., "Solar Cells: Operating Principles, Technology, and System Applications," Prentice-Hall, Englewood Cliffs NJ, 1982.
- Khan, F., Baek, S. H., Kim, J. H. (2016). Wide range temperature dependence of analytical photovoltaic cell parameters for silicon solar cells under high illumination conditions. *Applied Energy*, 183, 715-724.
- Mahfoud, A. (2015). Modélisation des cellules solaires tandem à couches minces et à haut rendement. PhD thesis, University of Sétif, Algeria
- Mahfoud, A., Mohamed, F., Mekhilef, S., Djahli, F. (2015). Effect of temperature on the GaInP/GaAs tandem solar cell performances. *International Journal of Renewable Energy Research*, 5(2), 629-634.
- Mallem, I. (2014). Simulation des cellules solaires hétérojonction Si-SiGe par SILVACO. Master thesis. University of Mohamed Khider Biskra Algeria.
- Manual, ATLAS User's Manual (2012). Device Simulation Software. Santa Clara, CA: SILVACO International
- Marouf, Y. (2013). Modélisation des cellules solaires en InGaN En utilisant Atlas Silvaco. Master Thesis, University of Mohamed Khider – Biskra Algeria.
- Mekemeche. A. (2017). Modélisation à deux dimensions des propriétés physiques de cellules solaires au silicium à base de substrat de type n. Étude de quelques cas particuliers de cellules innovantes. PhD thesis. University of Abd Hamid Ibn badis, Mostaganem.
- Quoizola, S. ( 2007). Epitaxie en phase vapeur de silicium sur silicium mésoporeux pour report sur substrats économiques et application photovoltaïque bas coût. PhD thesis. National Institute of applied sciences of Lyon.
- Sullivan, B. P. (2010). The effect of temperature on the optimization of photovoltaic cells using Silvaco ATLAS modelling. Master thesis. Naval Postgraduate School Monterey, California, USA.
- Terghini, O., Dehimi, L., Mefteh, A. M., & Bencherif, H. (2020). Performance evaluation and comparison of monolithic and mechanically stacked dual tandem InGaP/GaAs heterojunction on Ge Cell: A TCAD study. *Transactions on Electrical and Electronic Materials*, 21(4), 384-393.
- Zeghbrouck, V. (2007). Principles of Electronic Devices. University of Colorado (USA).